

TABLE 4-5 (cont.)  
CHEMISTRY PROPERTIES AND END-OF-LIFE KCU  
FOR WATTS BAR UNITS 1 AND 2

WNI	WC	WMN	WM	WCR	WST	WMD	WCB	CR(E)	NI(E)	CR/NI	DELTA	FRACTURE TOUGHNESS (KCU)
-----	----	-----	----	-----	-----	-----	-----	-------	-------	-------	-------	--------------------------

a,c,e

4-53

TABLE 4-5 (cont.)  
CHEMISTRY PROPERTIES AND END-OF-LIFE KCU  
FOR WATTS BAR UNITS 1 AND 2

SN1	SC	SNM	SM	%CR	%SI	%ND	%CB	CR(E)	NI(E)	CR/NI	DELTA	FRACTURE TOUGHNESS (KCU)
												a,c,e

4-14

TABLE 3 (cont.)  
CHEMISTRY PROPERTIES AND END-OF-LIFE KCU  
FOR WATTS BAR UNITS 1 AND 2

WNT	WC	WBN	WM	WCR	XSI	XND	XCB	CR(E)	NI(E)	CR/NI	DELTA	FRACTURE TOUGHNESS (KCU)
-----	----	-----	----	-----	-----	-----	-----	-------	-------	-------	-------	--------------------------

a,c,e

4-15

TABLE 4-5 (cont.)  
 CHEMISTRY PROPERTIES AND END-OF-LIFE KCU  
 FOR WATTS BAR UNITS 1 AND 2

WNI	WC	WMN	WM	WCR	WNI	WMD	WCB	CR(E)	NI(E)	CR/NI	DELTA	FRACTURE TOUGHNESS (KCU)
												a,c,e

4-16

TABLE 4-5 (cont.)  
 CHEMISTRY PROPERTIES AND END-OF-LIFE KCU  
 FOR WATTS BAR UNITS 1 AND 2

	%Ni	%C	%Mn	%N	%Cr	%Si	%Mo	%Cb	CR(E)	NI(E)	CR/NI	DELTA	FRACTURE TOUGHNESS (KCU)
													a,c,e

4-17

KEY: Delta - ferrite in percent weight  
 KCU - estimated Charpy U-notch energy for forty years service (daJ/cm<sup>2</sup>)

a,c,e



**Figure 4-1. Lower Bound True Stress Strain Curve for SA351-CF8A Stainless Steel at 558°F**

B,C,0

Figure 4-2. J vs  $\Delta a$  for a Cast Stainless Steel at 600°F



Figure 4-3. J vs.  $\Delta a$  at Different Temperatures for Aged Material  
: j<sup>S.C.</sup> (7500 Hours at 400°C)

## 5.0 LEAK RATE PREDICTIONS

### 5.1 Introduction

The next section on fracture evaluation will show that postulated through-wall cracks in the primary loop will remain stable and not cause a gross failure in the loop. If such a through-wall crack did exist, it would be desirable to detect the leakage such that the plant could be brought to a safe shutdown condition. The purpose of this section is to discuss the method which will be used to predict the flow through such a postulated crack and present the leak rate calculation results for through-wall circumferential cracks.

### 5.2 General Considerations

The flow of hot pressurized water through an opening to a lower back pressure causes flashing which can result in choking. For long channels where the ratio of the channel length,  $L$ , to hydraulic diameter,  $D_H$ , ( $L/D_H$ ) is greater than [ ]<sup>a,c,e</sup>, both [ ]<sup>a,c,e</sup> must be considered. In this situation the flow can be described as being single-phase through the channel until the local pressure equals the saturation pressure of the fluid. At this point, the flow begins to flash and choking occurs. Pressure losses due to momentum changes will dominate for [ ]<sup>a,c,e</sup>.

] <sup>a,c,e</sup>

### 5.3 Calculation Method

The basic method used in the leak rate calculations is the method developed by [

] <sup>a,c,e</sup>.

The flow rate through a crack was calculated in the following manner. Figure 5-1 from reference 5-1 was used to estimate the critical pressure,  $P_c$ , for the

primary loop enthalpy condition and an assumed flow. Once  $P_c$  was found for a given mass flow, the [ ]<sup>a,c,e</sup> was found from figure 5-2 taken from reference 5-1. For all cases considered, since [ ]<sup>a,c,e</sup>. Therefore, this method will yield the two-phase pressure drop due to momentum effects as illustrated in figure 5-3. Now using the assumed flow rate,  $G$ , the frictional pressure drop can be calculated using

$$\Delta P_f = [ ]^{a,c,e} \quad (5-1)$$

where the friction factor  $f$  is determined using the [ ]<sup>a,c,e</sup>. The crack relative roughness,  $\epsilon$ , was obtained from fatigue crack data on stainless steel samples. The relative roughness value used in these calculations was [ ]<sup>a,c,e</sup> RMS.

The frictional pressure drop using Equation 5-1 is then calculated for the assumed flow and added to the [ ]<sup>a,c,e</sup> to obtain the total pressure drop from the primary system to the atmosphere. That is, for the primary loop

$$\text{Absolute Pressure} - 14.7 = [ ]^{a,c,e} \quad (5-2)$$

for a given assumed flow  $G$ . If the right-hand side of Equation 5-2 does not agree with the pressure difference between the primary loop and the atmosphere, then the procedure is repeated until Equation 5-2 is satisfied to within an acceptable tolerance and this results in the flow value through the crack. This calculational procedure has been recommended by [ ]<sup>a,c,e</sup> for this type of [ ]<sup>a,c,e</sup> calculation.

#### 5.4 Leak Rate Calculations

Leak rate calculations were made as a function of crack length for the critical location previously identified. The normal operating loads of Table 3-2 were applied in these calculations. The crack opening area was estimated using the method of reference 5-3 and the average tensile properties established in section 4.2. The leak rate was calculated using the two-phase flow formulation described above. It was found that to obtain a flow rate of 10 gpm at normal operating conditions, a [ ]<sup>a,c,e</sup> inch long flaw would be required at location 10.

#### 5.5 References

5-1 [

] <sup>a,c,e</sup>,

5-2 [

] <sup>a,c,e</sup>

5-3 Tada, H., "The Effects of Shell Corrections on Stress Intensity Factors and the Crack Opening Area of Circumferential and a Longitudinal Through-Crack in a Pipe," Section II-1, NUREG/CR-3464, September 1983.

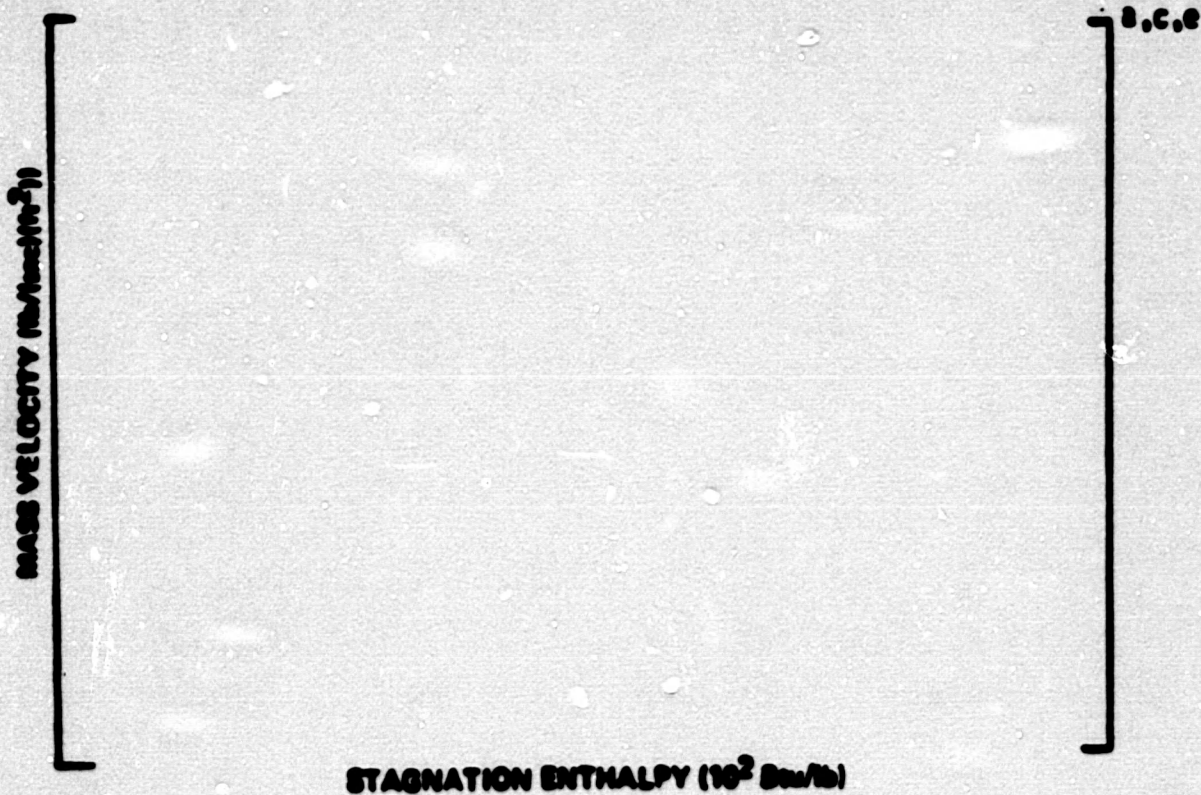


Figure 5-1. Analytical Predictions of Critical Flow Rates of Steam-Water Mixtures



Figure 5-2. [

] A.C.C. Pressure Ratio as a Function of L/D

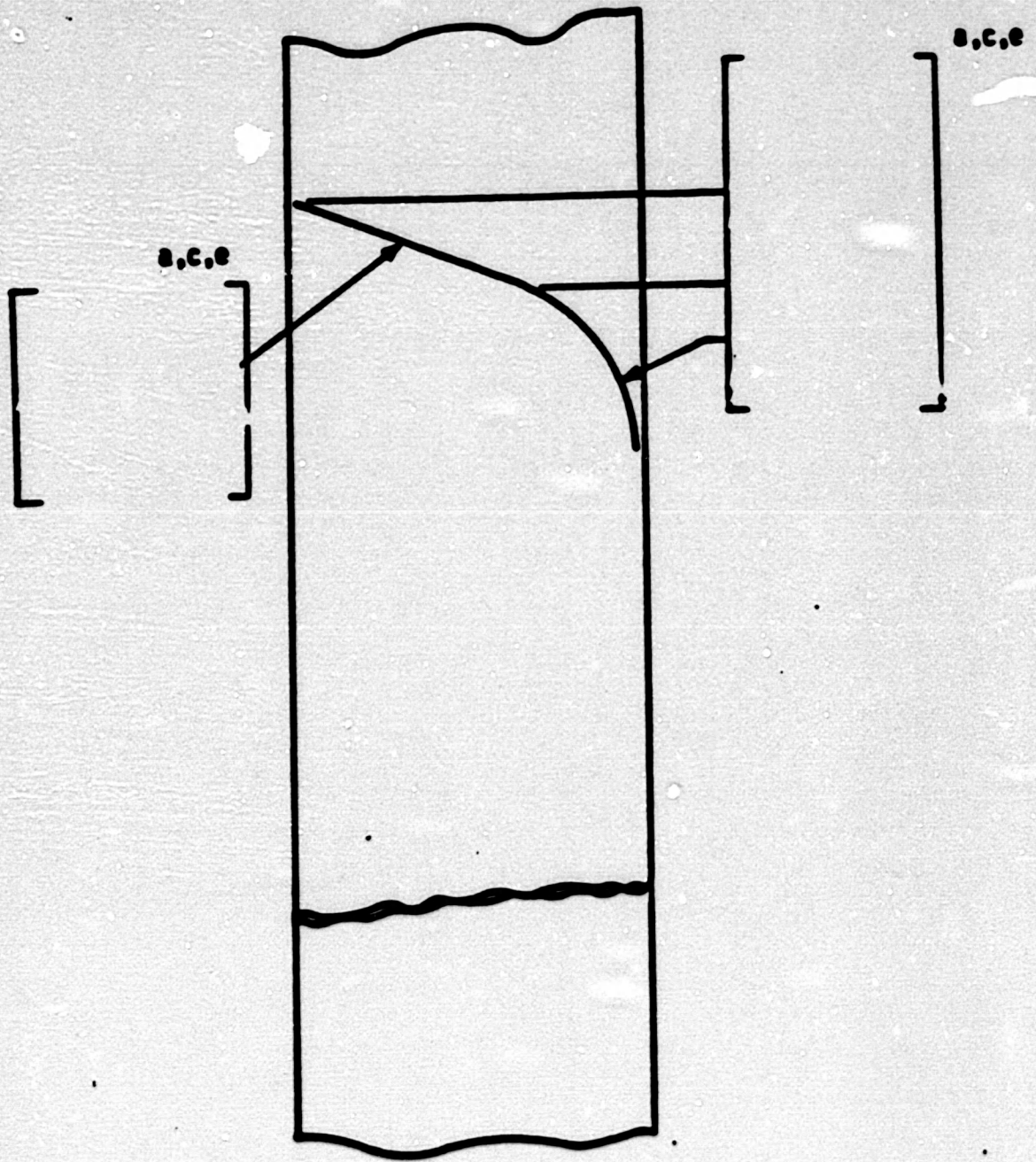


Figure 5-3. Idealized Pressure Drop Profile Through a Postulated Crack

## 6.0 FRACTURE EVALUATION

### 6.1 Global Stability Analysis

Determination of the conditions which lead to failure in stainless steel should be done with plastic fracture methodology because of the large amount of deformation accompanying fracture. One method for predicting the failure of ductile material is the plastic instability method, based on traditional plastic limit load concepts, but accounting for strain hardening and taking into account the presence of a flaw. The flawed pipe is predicted to fail when the remaining net section reaches a stress level at which a plastic hinge is formed. The stress level at which this occurs is termed as the flow stress. The flow stress is generally taken as the average of the yield and ultimate tensile strength of the material at the temperature of interest. This methodology has been shown to be applicable to ductile piping through a large number of experiments and will be used here to predict the critical flaw size in the primary coolant piping. The failure criterion has been obtained by requiring equilibrium of the section containing the flaw (figure 6-1) when loads are applied. The detailed development is provided in Appendix A for a through-wall circumferential flaw in a pipe with internal pressure, axial force, and imposed bending moments. The limit moment for such a pipe is given by:

$$[ \quad ]_{a,c,e}$$

where:

[

$$]_{a,c,e}$$

]a,c,e

The analytical model described above accurately accounts for the piping internal pressure as well as imposed axial force as they affect the limit moment. Good agreement was found between the analytical predictions and the experimental results (reference 6-1). Plots of limit moment versus crack length are given for location 10 in figure 6-2.

At location 10, the weld is of the SMAW category and therefore a correction factor for welds is applied to the loads (as recommended in reference 6-2) as follows:

$$Z = 1.15[1.0 + 0.013(OD-4)]$$

where OD is the outer diameter of the pipe in inches. A plot of limit moment versus crack length using the Z factor is given for location 10 in figure 6-3.

## 6.2 Local Stability Analysis

The local mechanism of failure is primarily dominated by the crack tip behavior in terms of crack-tip blunting, initiation, extension and finally crack instability. The stability will be assumed if the crack does not initiate at all. It has been accepted that the initiation toughness measured in terms of  $J_{IC}$  from a J-integral resistance curve is a material parameter defining the crack initiation. If, for a given load, the calculated J-integral value is shown to be less than the  $J_{IC}$  of the material, then the crack will not initiate. If the initiation criterion is not met, one can calculate the tearing modulus as defined by the following relation:

$$T_{app} = \frac{dJ}{da} \frac{E}{\sigma_f^2}$$

where:

$T_{app}$  = applied tearing modulus

$E$  = modulus of elasticity

$\sigma_f$  = [ ] (flow stress)

$a$  = crack length

a, c, e

The ductile tearing criterion is designated  $T_{mat}$  and is determined using the above formula from test results similar to those from which  $J_{Ic}$  is determined.

In summary, the crack stability will be established by the two-step criteria:

$$J < J_{Ic}$$

or

$$T_{app} < T_{mat} \text{ if } J \geq J_{Ic}$$

An additional supplementary criterion is that  $J \leq J_{max}$  is the maximum value of  $J$  associated with the  $dJ/da$  used to determine  $T_{mat}$  obtained from  $J$  tests for the material.

The values for  $J_{Ic}$ ,  $T_{mat}$  and  $J_{max}$  used in this report are given in section 4.3.

Using the stress-strain curves presented in section 4.0, elastic-plastic fracture mechanics (EPFM) J-integral analyses for through-wall circumferential cracks in a cylinder were performed for critical location 10 using the procedure in the EPRI fracture mechanics handbook (reference 6-3). For the critical location, a flaw size of twice the length required to allow a 10 gpm leak rate was used. Faulted condition loadings were applied.

### 6.3 Results of Crack Stability Evaluation

In this section, the results of the stability calculations described in sections 6.1 and 6.2 are discussed in further detail.

Figure 6-2 shows a plot of the plastic limit moment as a function of through-wall circumferential flaw length in the cold leg of the main coolant piping (critical location 10.) This limit moment was calculated for Watts Bar Units 1 and 2 from data for a pressurized pipe at 2305 psi with an axial force of 2008 kips, (including the pressure) operating at 558°F with appropriate minimum base metal tensile properties. The maximum applied bending moment of 23468 in-kips can be plotted on this figure and used to determine a critical flaw length, which is shown to be [ ]<sup>a,c,e</sup> inches.

Figure 6-3 shows a plot of the limit moment versus circumferential flaw length at location 10 when the Z factor for the SMAW weld is incorporated. Here, a maximum applied moment of 36856 in-kips (Z x 23468) gives a [ ]<sup>a,c,e</sup> inch critical flaw length for the weld. Noting that the flaw yielding a leakage of 10 gpm (leakage size flaw) was calculated to be [ ]<sup>a,c,e</sup> inches long (section 6) a factor of over 4 exists between the leakage size flaw and the critical flaw obtained by global analysis with "Z" factor correction.

The results for the local stability analysis show that for location number 10, the applied J is [ ]<sup>a,c,e</sup> in-lb/in<sup>2</sup> with a T of [ ]<sup>a,c,e</sup> for a [ ]<sup>a,c,e</sup> inch long crack. Thus, T<sub>applied</sub> [ ]<sup>a,c,e</sup> is less than T<sub>mat</sub> [ ]<sup>a,c,e</sup> and J<sub>applied</sub> [ ]<sup>a,c,e</sup> in-lb/in<sup>2</sup> is less than J<sub>max</sub> [ ]<sup>a,c,e</sup> in-lb/in<sup>2</sup>. Therefore, the postulated [ ]<sup>a,c,e</sup> inches long flaw would remain stable. As was

shown in section 5.0, a 4.8 inch long crack will yield a 10 gpm leakage rate when subjected to normal operating loads. Therefore a margin of 2 with respect to flaw size is evident.

The loads used in the flaw stability evaluation described above were obtained by absolute combination of the individual components as described in section 3.2. Therefore, as recommended by SRP 3.6.3, the required margin on load of 1.0 is also accomplished.

#### 6.4 References

6-1 Kanninen, M. F., et. al., "Mechanical Fracture Predictions for Sensitized Stainless Steel Piping with Circumferential Cracks," EPRI NP-192, September 1976.

6-2 Pressure Vessel and Piping Codes, ASME, Journal of Pressure Vessel Technology, August 1986, Volume 108.

6-3 Kumar, V., German, M. D. and Shih, C. P., "An Engineering Approach for Elastic-Plastic Fracture Analysis," EPRI Report NP-1931, Project 1237-1, Electric Power Research Institute, July 1981.

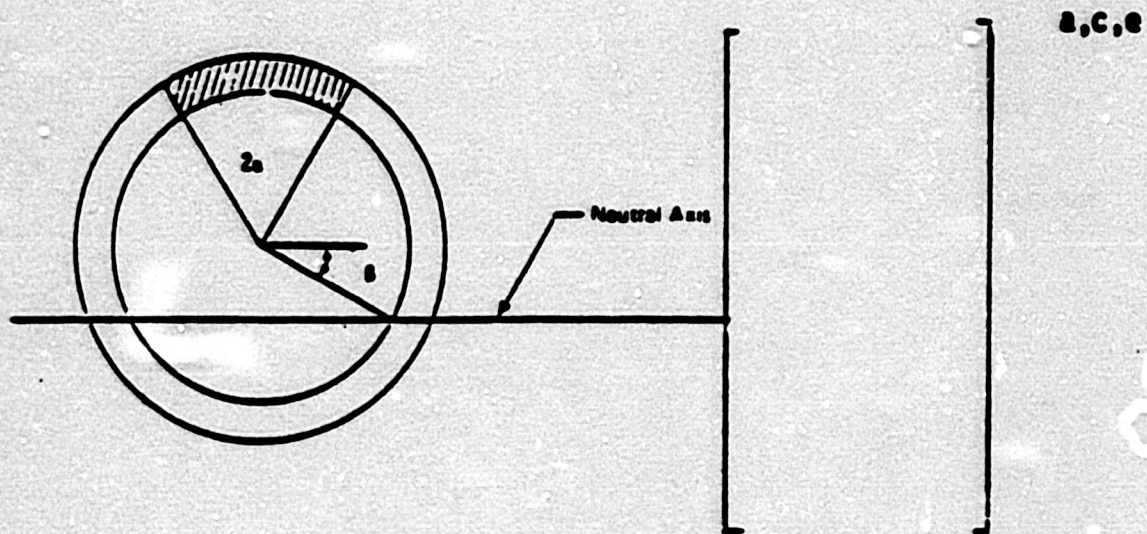
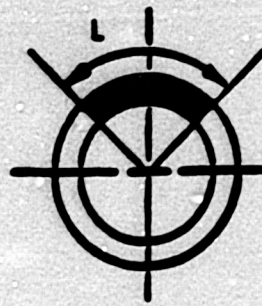


Figure 6-1. [

]  $a, c, e$  Stress Distribution

S.C.8



FLAW GEOMETRY

OD = 32.13 inches

t = 2.21 inches

F = 2008 kips

$\sigma_y = 21.09$  ksi

$\sigma_u = 58.25$  ksi

$\sigma_f = 39.67$  ksi

Figure 6-2. Critical Flaw Size Prediction - Cold Leg at Critical Location 10

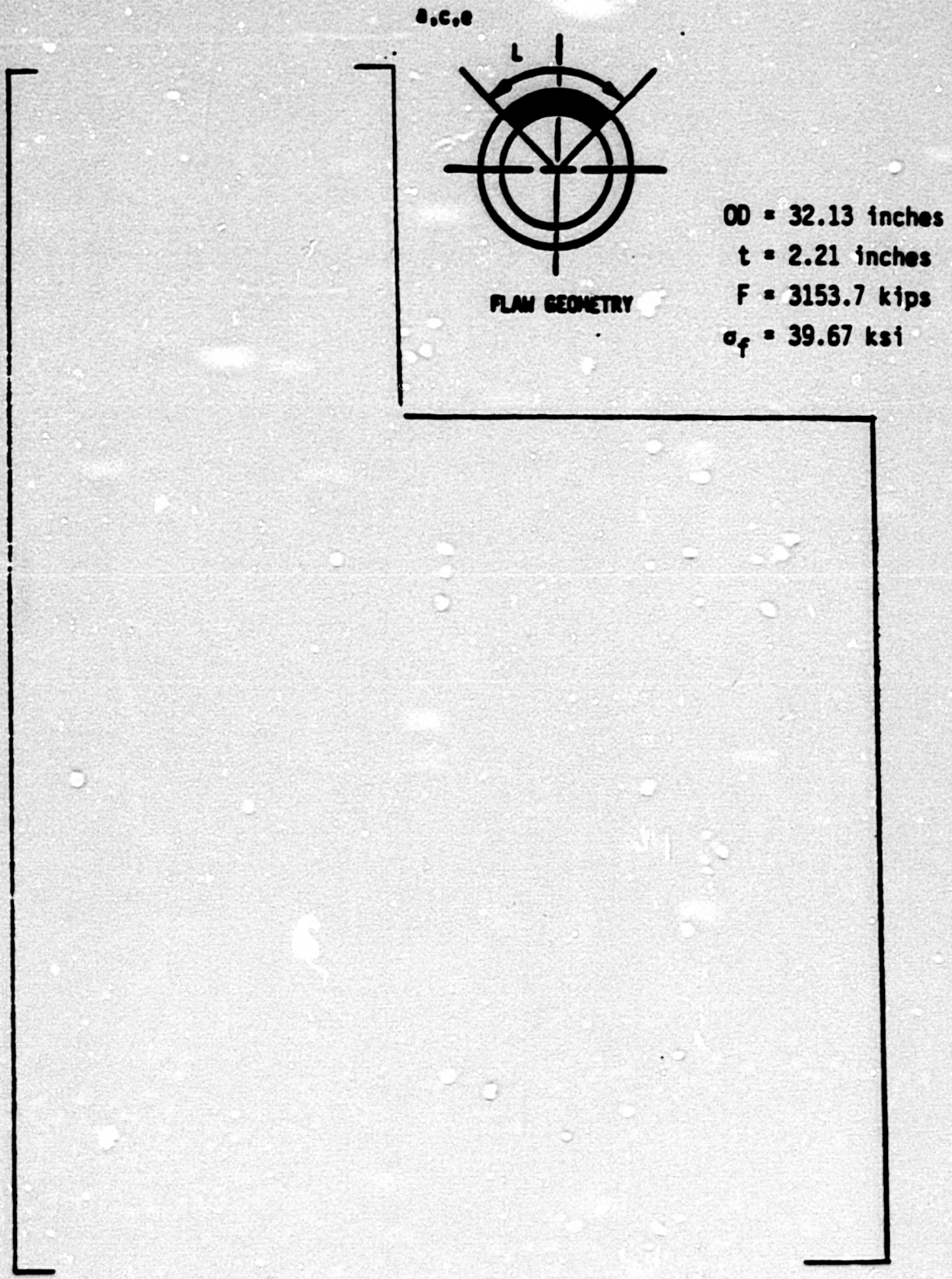


**Figure 6-3. Z-Factor Calculations for SMAW Welds to Demonstrate Margin on Flaw Size at Location 10**

## 7.0 FATIGUE CRACK GROWTH ANALYSIS

### 7.1 Acceptability of Fatigue Crack Growth

To determine the sensitivity of the primary coolant system to the presence of small cracks, a fatigue crack growth analysis was carried out for the [ ]<sup>a,c,e</sup> region of a typical system (see Location [ ]<sup>a,c,e</sup> of figure 3-2). This region was selected because crack growth calculated here will be typical of that in the entire primary loop. Crack growths calculated at other locations can be expected to show less than 10% variation. Thermal aging has been shown not to impact fatigue crack growth (references 7-1 and 7-2).

A [ ]<sup>a,c,e</sup> of a plant typical in geometry and operational characteristics to any Westinghouse PWR System. [ ]

[ ]<sup>a,c,e</sup> All normal, upset, and test conditions were considered and circumferentially oriented surface flaws were postulated in the region, assuming the flaw was located in three different locations, as shown in Figure 7-1. Specifically, these were:

Cross Section A: [ ]<sup>a,c,e</sup>  
Cross Section B: [ ]<sup>a,c,e</sup>  
Cross Section C: [ ]<sup>a,c,e</sup>

The fatigue crack growth (FCG) analyses were conducted in the same manner as suggested by Section XI, Appendix A of the ASME Boiler and Pressure Vessel Code.

Fatigue crack growth rate laws were used [ ]

[ ]<sup>a,c,e</sup> The law for stainless steel

was derived from reference 7-3, with a very conservative correction for the R ratio, which is the ratio of minimum to maximum stress during a transient. For stainless steel, the fatigue crack growth formula is:

$$\frac{da}{dn} = (5.4 \times 10^{-12}) K_{eff}^{4.48} \text{ inches/cycle}$$

where  $K_{eff} = K_{max} (1-R)^{0.5}$

$$R = K_{min}/K_{max}$$

[

]a,c,e

[

]a,c,e

where: [ ]a,c,e

The calculated fatigue crack growth for semi-elliptic surface flaws of circumferential orientation and various depths is summarized in table 7-1, and shows that the crack growth is very small, regardless [ ]a,c,e

## 7.2 References

7-1 WCAP-10456, "The Effects of Thermal Aging on the Structural Integrity of Cast Stainless Steel Piping for W N<sub>2</sub>SS," W Proprietary Class 2, November 1983.

7-2 Slama, G., Petrequin, P., Masson, S. H., and Mager, T. R., "Effect of Aging on Mechanical Properties of Austenitic Stainless Steel Casting and Welds," presented at SMiRT 7 Post Conference Seminar 6 - Assuring Structural Integrity of Steel Reactor Pressure Boundary Components, August 29/30, 1983, Monterey, CA.

7-3 Bamford, W. H., "Fatigue Crack Growth of Stainless Steel Piping in a Pressurized Water Reactor Environment," Trans. ASME Journal of Pressure Vessel Technology, Vol. 101, Feb. 1979.

7-4 [

]a,c,e

7-5 [

]a,c,e

TABLE 7-1

FATIGUE CRACK GROWTH AT [

] <sup>a,c,e</sup> (40 YEARS)

INITIAL FLAW (IN)	FINAL FLAW (in)		
	[ <sup>a,c,e</sup>	[ <sup>a,c,e</sup>	[ <sup>a,c,e</sup>
0.292	0.31097	0.30107	0.30698
0.300	0.31949	0.30953	0.31626
0.375	0.39940	0.38948	0.40763
0.425	0.45271	0.4435	0.47421

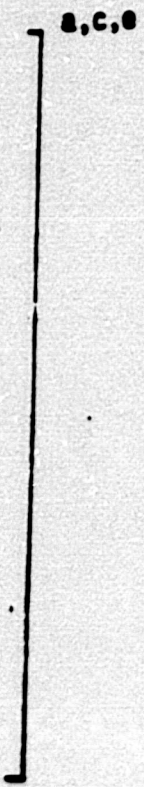


Figure 7-1. Typical Cross-Section of [

]A.C.O

CRACK GROWTH RATE,  $da/dN$  (MICRO-INCHES/CYCLE)

A.C. 0

STRESS INTENSITY FACTOR RANGE ( $\Delta K_I$  (KSI $\sqrt{IN.}$ )

Figure 7-2. Reference Fatigue Crack Growth Curves for [  
A.C. 0

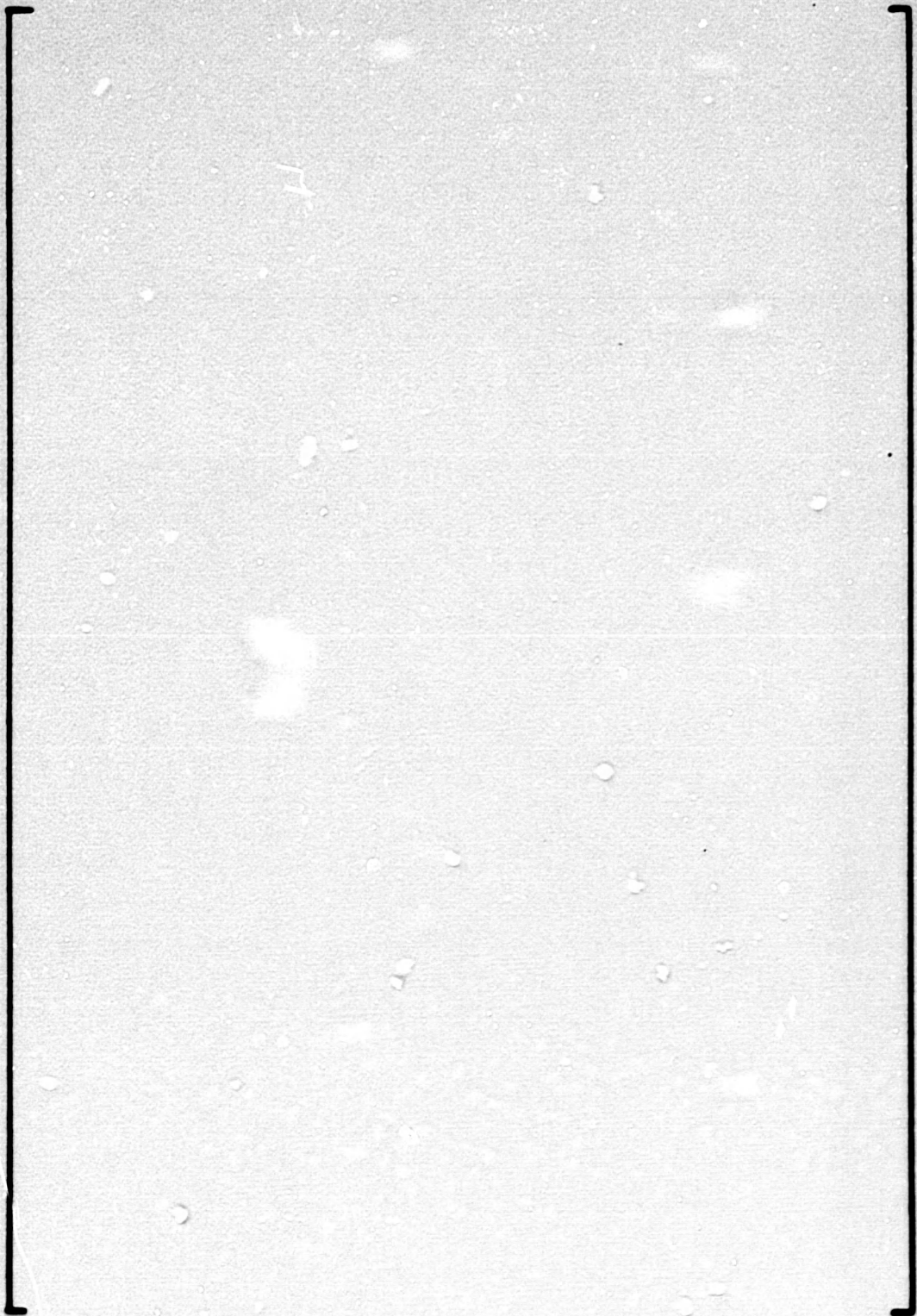


Figure 7-3. Reference Fatigue Crack Growth Law for [ in a Water Environment at 600°F

]a.c.e

## 8.0 ASSESSMENT OF MARGINS

In the preceding sections, the leak rate calculations, fracture mechanics analyses and fatigue crack growth assessments were performed. Margins are discussed below.

At the governing location 10 the flaw size yielding a leak rate of 10 gpm (i.e. "leakage size flaw" or "reference flaw") when subjected to normal operating loads is found to be [ ]<sup>a,c,e</sup> inches long.

The critical flaw size at the governing location using the limit load approach is found to be [ ]<sup>a,c,e</sup> inches. Using the ASME Section XI, IWB-3640 approach (also called the Z factor approach) for the SMAW weld, the critical flaw size is found to be [ ]<sup>a,c,e</sup> inches long.

Local crack stability has also been demonstrated with required margins. At location 10, a [ ]<sup>a,c,e</sup> inch long flaw (which is twice the flaw length giving 10 gpm leakage at normal operating conditions) subjected to faulted loads resulted in  $J_{\text{applied}}$  of [ ]<sup>a,c,e</sup> in-lb/in<sup>2</sup>, which is less than the 3000 in-lb/in<sup>2</sup> allowed. Thus, a margin of 10 on leak rate and a margin of 2 on flaw size is demonstrated.

In summary, relative to

### 1. Flaw Size

- a. A margin of at least 2 exists between the critical flaw and the flaw yielding a leak rate of 10 gpm.
- b. If limit load is used as the basis for critical flaw size, a larger margin for global stability would result.

## 2. Leak Rate

A margin of 10 exists for the reference flaws between calculated leak rate and the 1 gpm leak detection capability of the Watts Bar plants.

## 3. Loads

- a. The  $J_{app}$  values for the Watts Bar plants are enveloped by the toughness allowables established for thermally aged material.
- b. At the governing location the leakage size flaw was shown to be stable when subjected to normal plus SSE loads obtained by absolute summation of individual components. This method of combination results in maximum load at the location of interest.

## 9.0 CONCLUSIONS

This report justifies the elimination of RCS primary loop pipe breaks for the Watts Bar Units 1 and 2 plants as follows:

- a. Stress corrosion cracking is precluded by use of fracture resistant materials in the piping system and controls on reactor coolant chemistry, temperature, pressure, and flow during normal operation.
- b. Water hammer should not occur in the RCS piping because of system design, testing, and operational considerations.
- c. The effects of low and high cycle fatigue on the integrity of the primary piping are negligible.
- d. Ample margin exists between the leak rate of small stable flaws and the capability of the Watts Bar plants' reactor coolant system pressure boundary leakage detection system.
- e. Ample margin exists between the small flaw of item d and larger stable flaws.
- f. Ample margin exists in the material properties used to demonstrate end-of-service life (relative to aging) stability of the critical flaws.

Based on the above, it is concluded that RCS primary loop pipe breaks need not be considered in the structural design basis of Watts Bar Units 1 and 2.

APPENDIX A

] a.c.o



**Figure A-1. Pipe With a Through-Wall Crack in Bending**

**Enclosure 2**

**Westinghouse Electric Corporation, "Technical Justification for Eliminating Large Primary Loop Pipe Rupture as the Structural Design Basis for Watts Bar Units 1 and 2," dated November 1988; WCAP-11985, proprietary version.**